Shortcuts to adiabatic passage for population transfer and maximum entanglement creation between two atoms in a cavity

Mei Lu,[1] Yan Xia,[1,*] Li-Tuo Shen,[1] Jie Song,[2,†] and Nguyen Ba An[3,‡]

[1]*Department of Physics, Fuzhou University, Fuzhou 350108, China*

[2]*Department of Physics, Harbin Institute of Technology, Harbin 150001, China*

[3]*Center for Theoretical Physics, Institute of Physics, Vietnam Academy of Science and Technology, 18 Hoang Quoc Viet,*

Cau Giay, Hanoi, Vietnam

We use the approach of "transitionless quantum driving" proposed by Berry to construct shortcuts to the population transfer and the creation of maximal entanglement between two Λ-type atoms based on the cavity quantum electronic dynamics system. An effective Hamiltonian is designed by resorting to an auxiliary excited level, a classical driving field, and an extra cavity field mode to supplement or substitute the original reference Hamiltonian, and steer the system evolution along its instantaneous eigenstates in an arbitrarily short time, speeding up the rate of population transfer and creation of maximal entanglement between the two atoms inside a cavity. Numerical simulation demonstrates that our shortcuts are robust against the decoherences caused by atomic spontaneous emission and cavity photon leakage.

I. INTRODUCTION

Controlling the dynamics of quantum systems is of crucial importance for many practical purposes. A widely used method is to drive the system with external time-dependent interactions, making the total Hamiltonian $H_0(t)$ depend explicitly on time. The change in time is managed to be slow to allow adiabatic passage from an initial state to a target state. Under the adiabatic following condition, it is likely that the instantaneous eigenstates of $H_0(t)$ are the moving states. That is, each evolves along itself all the time without transition to other ones [1].

However, that is not precise. In fact, transitions between different time-dependent instantaneous eigenstates may still happen with nonzero probabilities which become nonnegligible if the controlling parameters do not change slowly enough, reducing fidelity of the evolved state with respect to the target one. Thus, controlling quantum states based on adiabatic passage is by its nature a long process [2]. If the required evolution time is too long, the method may be useless, because decoherence, noise, or losses would spoil the intended dynamics. This limits application ranges in practice, especially in the field of quantum computing and quantum-information processing where speed is of primary concern. Therefore, accelerating the dynamics towards the perfect final outcome is a nice idea and perhaps the most reasonable way to actually fight against the decoherence, noise, or losses that are accumulated during a long operation time.

So far various schemes for shortcuts to slow an adiabatic passage method for arriving at a target state from an initial state have been proposed in theory [3–20] and implemented in experiment [21–26]. To be useful, such nonadiabatic shortcuts must, of course, be reliable, fast, and robust.

Notably, as pointed out by Berry [1], a nearly Hamiltonian $H(t)$, which is associated with any given reference Hamiltonian $H_0(t)$, exists that derives instantaneous eigenstates of $H_0(t)$ exactly, i.e., transitions between them do not occur at all during the whole duration of system evolution regardless of the rate of change. In other words, the instantaneous eigenstates of $H_0(t)$ can be regarded as truly moving eigenstates of $H(t)$. Because of such feature of the driving, Berry called it "transitionless quantum driving" and $H(t)$ the "counter-diabatic driving" (CDD) Hamiltonian. More importantly, Berry also worked out a general "transitionless tracking algorithm" to reverse engineer $H(t)$ from $H_0(t)$. Recently, transitionless quantum drivings in Berry's spirit have been experimentally demonstrated in the effective two-level system [26]. Furthermore, Chen *et al.* [14] have also put forward another reverse-engineering approach using the Lewis-Riesenfeld (LR) invariant to carry the eigenstates of a Hamiltonian from a specified initial to a final configuration, then to design the transient Hamiltonian from the LR invariant. Although different in form, those driving methods are shown to be essentially equivalent to each other by properly adjusting the reference Hamiltonian [15].

It is worth noticing that although the reverse-engineering approach has been applied to achieve accelerated population transfer between two internal states of a single atom in different systems, fast population transfer between two atoms inside a common environment has not been studied adequately, to our knowledge. In view of the requirements for scalable quantum computing and quantum-information processing, it is desirable to extend the approach to multi-qubit systems. In this context, the LR invariant approach for ultrafast quantum-state transfer between two Λ-type atoms based on the cavity quantum electronic dynamics (CQED) system has just been studied in [20].

In this paper, we present an alternative nonadiabatic proposal to speed up the population transfer and the creation of maximal entanglement between two atoms inside a cavity in the spirit of Berry's transitionless quantum driving approach. Different from the previous schemes [14–18] where the CDD Hamiltonian derived from the original reference Hamiltonian can be realized experimentally in terms of a time-dependent magnetic field between two levels of a single atom, in our

————
*xia-208@163.com
†jsong@hit.edu.cn
‡nban@iop.vast.ac.vn

system with two atoms in a common cavity the reverse engineered CDD Hamiltonian is not readily available within the model under consideration. To circumvent this, we take into account one more auxiliary excited level for each atom, an extra external laser field, and an extra cavity field mode to experimentally realize our shortcut schemes to adiabatic passage and construct the auxiliary interaction Hamiltonian that provides us with the extra shortcut interaction. Though the extra shortcut interaction derived from the reference Hamiltonian can speed up the population transfer and the rate of maximally entangled state creation, the perfect shortcut performance is slightly deteriorated since the derivation of the auxiliary effective Hamiltonian is based on the large detuning condition. Still, our extra shortcut interaction can considerably accelerate the slow adiabatic passage and the performance based on it is robust, thus promising to be realized experimentally.

Our paper is structured as follows. In Sec. II, we describe the theoretical model for two Λ-type atoms embedded in a single-mode cavity. In Sec. III, we construct a shortcut passage for population transfer between two atoms. In Sec. IV, the shortcut for generating maximal entanglement between two atoms is achieved. In Sec. V, the influences of decoherence on the shortcut for population transfer and maximal entanglement generation are considered. The conclusion appears in Sec. VI.

II. MODEL

The model we consider consists of two Λ-type atoms embedded in a single-mode cavity, as sketched by solid bars and solid arrows in Fig. 1. The transitions $|g\rangle_1 \leftrightarrow |s\rangle_1$ and $|g\rangle_2 \leftrightarrow |s\rangle_2$ are resonantly driven by two time-dependent classical fields $\Omega_1(t)$ and $\Omega_2(t)$, which are $3\pi/2$-dephased from each other, while each transition $|f\rangle_i \leftrightarrow |s\rangle_i$ ($i = 1,2$) is resonantly coupled to a cavity mode with a coupling constant g_i. Under the rotating-wave approximation (RWA), the time-dependent interaction Hamiltonian for the whole system reads ($\hbar = 1$):

$$H_0(t) = \Omega_1(t)|s\rangle_1\langle g| - i\Omega_2(t)|s\rangle_2\langle g|$$
$$+ \sum_{i=1,2} g_i a|s\rangle_i\langle f| + \text{H.c.}, \qquad (1)$$

where a is the annihilation operator of the cavity mode.

If the initial state is $|g\rangle_1|f\rangle_2|0\rangle_c$, with $|0\rangle_c$ being the vacuum state of the cavity, the whole system evolves within a single-excitation subspace spanned by five basic states

$$|\phi_1\rangle = |g\rangle_1|f\rangle_2|0\rangle_c, \qquad (2)$$

$$|\phi_2\rangle = |s\rangle_1|f\rangle_2|0\rangle_c, \qquad (3)$$

$$|\phi_3\rangle = |f\rangle_1|f\rangle_2|1\rangle_c, \qquad (4)$$

$$|\phi_4\rangle = |f\rangle_1|s\rangle_2|0\rangle_c, \qquad (5)$$

and

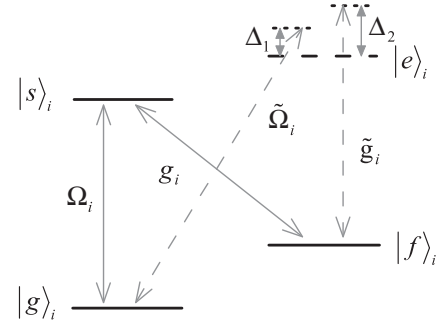$$|\phi_5\rangle = |f\rangle_1|g\rangle_2|0\rangle_c. \qquad (6)$$

FIG. 1. Λ-type configuration for the ith atom consists of one excited state $|s\rangle_i$ and two ground states $|g\rangle_i$ and $|f\rangle_i$. The transition $|g\rangle_i \leftrightarrow |s\rangle_i$ is resonantly driven by a time-dependent classical field with Rabi frequency $\Omega_i(t)$, while $|f\rangle_i \leftrightarrow |s\rangle_i$ is resonantly coupled to a cavity mode a with a coupling constant g_i. The auxiliary excited state $|e\rangle_i$ is nonresonantly coupled to $|g\rangle_i$ by a time-dependent classical field with Rabi frequency $\tilde{\Omega}_i(t)$ and to $|f\rangle_i$ by a cavity mode b with a coupling constant $\tilde{g}_i$. $\Delta_{1,2}$ are finite detunings.

We assume $g_i = g$ in this paper for simplicity. For our purposes we also assume the weak-driving fields specified by

$$|\Omega_{1,2}(t)| \ll g. \qquad (7)$$

Then, at an instant time t the eigenstates $|\psi_n(t)\rangle$ and eigenvalues $\lambda_n(t)$ of $H_0(t)$, which obey the equation $H_0(t)|\psi_n(t)\rangle = \lambda_n(t)|\psi_n(t)\rangle$, can be derived analytically. For the former,

$$|\psi_1(t)\rangle = \left(\Omega_1^2(t) + \Omega_2^2(t) + \frac{\Omega_1^2(t)\Omega_2^2(t)}{g^2}\right)^{-1/2}$$
$$\times\left(-i\Omega_2(t)|\phi_1\rangle + \frac{i\Omega_1(t)\Omega_2(t)}{g}|\phi_3\rangle + \Omega_1(t)|\phi_5\rangle\right), \qquad (8)$$

$$|\psi_2(t)\rangle \simeq \frac{i\Omega_1(t)}{\sqrt{2[\Omega_1^2(t) + \Omega_2^2(t)]}}|\phi_1\rangle - \frac{i}{2}|\phi_2\rangle$$
$$+ \frac{i}{2}|\phi_4\rangle + \frac{\Omega_2(t)}{\sqrt{2[\Omega_1^2(t) + \Omega_2^2(t)]}}|\phi_5\rangle, \qquad (9)$$

$$|\psi_3(t)\rangle \simeq \frac{i\Omega_1(t)}{\sqrt{2[\Omega_1^2(t) + \Omega_2^2(t)]}}|\phi_1\rangle + \frac{i}{2}|\phi_2\rangle$$
$$- \frac{i}{2}|\phi_4\rangle + \frac{\Omega_2(t)}{\sqrt{2[\Omega_1^2(t) + \Omega_2^2(t)]}}|\phi_5\rangle, \qquad (10)$$

$$|\psi_4(t)\rangle \simeq \left(\frac{\Omega_1^2(t) + \Omega_2^2(t)}{g^2} + 8\right)^{-1/2}$$
$$\times\left(-i\frac{\Omega_1(t)}{g}|\phi_1\rangle + i\sqrt{2}|\phi_2\rangle\right.$$
$$\left. - 2i|\phi_3\rangle + i\sqrt{2}|\phi_4\rangle + \frac{\Omega_2(t)}{g}|\phi_5\rangle\right), \qquad (11)$$

and

$$|\psi_5(t)\rangle \simeq \left(\frac{\Omega_1^2(t) + \Omega_2^2(t)}{g^2} + 8\right)^{-1/2}$$
$$\times \left(-i\frac{\Omega_1(t)}{g}|\phi_1\rangle - i\sqrt{2}|\phi_2\rangle \right.$$
$$\left. - 2i|\phi_3\rangle - i\sqrt{2}|\phi_4\rangle + \frac{\Omega_2(t)}{g}|\phi_5\rangle\right), \quad (12)$$

and, for the latter, $\lambda_1 = 0$, $\lambda_2 \simeq -\sqrt{[\Omega_1^2(t) + \Omega_2^2(t)]/2}$, $\lambda_3 \simeq \sqrt{[\Omega_1^2(t) + \Omega_2^2(t)]/2}$, $\lambda_4 \simeq -\sqrt{2}g$, and $\lambda_5 \simeq \sqrt{2}g$, respectively. Note that the eigenstate $|\psi_1(t)\rangle$ with zero eigenvalue $\lambda_1 = 0$ is a dark state.

Here, starting from the atomic state $|g\rangle_1|f\rangle_2$, we are concerned with two problems. The first problem is how to transfer population simultaneously in the two atoms, i.e., $|g\rangle_1 \rightarrow |f\rangle_1$ and $|f\rangle_2 \rightarrow |g\rangle_2$, or, in other words, how to drive the two atoms from the initial state $|g\rangle_1|f\rangle_2$ to the target state $|f\rangle_1|g\rangle_2$. The second problem is how to create maximum entanglement between the two atoms. As is well known, the adiabatic passage method does well with these problems. Namely, when the adiabatic condition [2] $|\langle\psi_{n\neq1}(t)|\partial_t\psi_1(t)\rangle| \ll |\lambda_{n\neq1}|$, with $\partial_t \equiv \partial/\partial t$, is satisfied, state $|\psi_1(0)\rangle$ would follow $|\psi_1(t)\rangle$ closely. This assumption in Eq. (7) neglects the probability of populating state $|\phi_3\rangle$ during the entire process of evolution. Then, by judiciously tailoring the classical fields $\Omega_1(t)$ and $\Omega_2(t)$, either of the two above-mentioned problems can be solved successfully. Although the adiabatic passage method is one-step implementation, it usually takes quite a long time, which is undesirable. If one attempts to quicken the process a little bit, the adiabatic following condition may be violated and transition to states other than $|\psi_1(t)\rangle$ may happen, leading to a wrong (unintended) final state. In the next sections we shall consider fast and robust shortcuts to adiabaticity for the two above problems.

III. SHORTCUT FOR SIMULTANEOUS POPULATION TRANSFER IN TWO ATOMS

Because the instantaneous eigenstates $\{|\psi_n(t)\rangle\}$, Eqs. (8)–(12), are not solutions of the Schrodinger equation $i\partial_t|\psi_n(t)\rangle = H_0(t)|\psi_n(t)\rangle$, there is a finite, though small, probability that the system starts from state $|\psi_n(0)\rangle$ and ends up in state $|\psi_{m\neq n}(t)\rangle$, even under the adiabatic following condition. To guarantee zero transition probability for $|\psi_n(0)\rangle \rightarrow |\psi_{m\neq n}(t)\rangle$, we look for a Hamiltonian $H(t)$ that is related to the original Hamiltonian $H_0(t)$ but drives the eigenstates $\{|\psi_n(t)\rangle\}$ exactly, i.e., $i\partial_t|\psi_n(t)\rangle = H(t)|\psi_n(t)\rangle$.

According to Berry's general transitionless tracking algorithm [1], one can reverse engineer $H(t)$ from $H_0(t)$. The algorithm results in infinitely many such Hamiltonians $H(t)$ which differ from each other only by phases. Disregarding the effect of phases, the simplest Hamiltonian $H_1(t)$ that exactly drives the set of instantaneous eigenstates of $H_0(t)$ is derived in the form

$$H_1(t) = i\sum_{m=1}^{5}|\partial_t\psi_m(t)\rangle\langle\psi_m(t)|. \quad (13)$$

The addition of $H_0(t)$ to $H_1(t)$ [i.e., $H(t) = H_0(t) + H_1(t)$] only affects the phases of the system evolution. Being interested only in populations, we can exclude $H_0(t)$ [i.e., $H(t) = H_1(t)$]. Putting Eqs. (8)–(12) into Eq. (13), we obtain, after differentiating each of the $|\psi_n(t)\rangle$ and then summing up all five terms, the following expression for $H_1(t)$:

$$H_1(t) = C(t)(|\phi_1\rangle\langle\phi_5| + |\phi_5\rangle\langle\phi_1|), \quad (14)$$

where

$$C(t) = \frac{\Omega_1(t)\partial_t\Omega_2(t) - \Omega_2(t)\partial_t\Omega_1(t)}{\Omega_1^2(t) + \Omega_2^2(t) + \Omega_1^2(t)\Omega_2^2(t)/g^2}. \quad (15)$$

We remark, however, that for two Λ-type atoms in a real experiment, the CDD Hamiltonian $H_1(t)$ in Eq. (14) does not exist. Therefore, we shall find an alternative physically feasible Hamiltonian which is equivalent to $H_1(t)$. Generally, the physical realization of such Hamiltonians is case dependent. For example, in Chen's scheme [14] for nonadiabatic speeding up the population transfer in two- and three-level systems of a single atom, an auxiliary laser or microwave interactions are involved to directly drive two internal levels of the atom. Here we take into account an auxiliary excited level $|e\rangle_i$, additional classical driving fields $\tilde{\Omega}_i(t)$ and an extra cavity field mode to realize an equivalent-to-the-CDD Hamiltonian that indirectly drives the two interested states $|\phi_1\rangle$ and $|\phi_5\rangle$, as shown by dashed bars and dashed arrows in Fig. 1. The transition $|f\rangle_i \leftrightarrow |e\rangle_i$ is dispersively coupled to the auxiliary cavity mode with a real coupling constant $\tilde{g}_i$ and a detuning Δ_2, while $|g\rangle_i$ is nonresonantly coupled to $|e\rangle_i$ by a laser field with a Rabi frequency $\tilde{\Omega}_i(t)$ and a detuning Δ_1. Under the RWA, the auxiliary interaction Hamiltonian is ($\hbar = 1$)

$$\tilde{H}(t) = \sum_{i=1}^{2}[\tilde{\Omega}_i(t)e^{i\Delta_1 t}|g\rangle_i\langle e| + \tilde{g}_ie^{i\Delta_2 t}b^\dagger|f\rangle_i\langle e| + \text{H.c.}],$$
$$(16)$$

where $b^\dagger$ is the creation operation for the auxiliary cavity mode. We assume $\tilde{g}_i = g$ and $\tilde{\Omega}_i(t) = \tilde{\Omega}(t)$ in this paper for simplicity.

Let the system be initially in state $|\phi_1\rangle$. In the large detuning regime $\Delta_1, \Delta_2 \gg \tilde{\Omega}(t), g$, and $|\delta| \equiv |\Delta_1 - \Delta_2| \gg \eta(t) \equiv \frac{1}{2}(\frac{1}{\Delta_1} + \frac{1}{\Delta_2})g\tilde{\Omega}(t)$, the atoms can mutually exchange energy in such a way that the level $|e\rangle$ and the auxiliary cavity field mode b are only virtually excited [27,28]. Then $\tilde{H}(t)$ can effectively be described by the Hamiltonian

$$\tilde{H}_{\text{eff}}(t) = \frac{\eta^2(t)}{\delta}(S_1^+ S_2^- + S_2^+ S_1^-), \quad (17)$$

where $S_j^+ = |f\rangle_j\langle g|$ and $S_j^- = |g\rangle_j\langle f|$, with $j = 1,2$. The effective Hamiltonian (17) is equivalent with the CDD Hamiltonian $H_1(t)$ in Eq. (14) when

$$\frac{\eta^2(t)}{\delta} = C(t). \quad (18)$$

Hence, the Rabi frequency of the auxiliary laser field that generates a Hamiltonian equivalent to the CDD Hamiltonian can be determined from the original frequencies $\Omega_1(t)$ and $\Omega_2(t)$ as

$$\tilde{\Omega}(t) = \frac{2\Delta_1\Delta_2}{\Delta_1 + \Delta_2}\sqrt{\frac{[\Omega_1(t)\partial_t\Omega_2(t) - \Omega_2(t)\partial_t\Omega_1(t)]\delta}{[\Omega_1^2(t) + \Omega_2^2(t)]g^2 + \Omega_1^2(t)\Omega_2^2(t)}}. \quad (19)$$
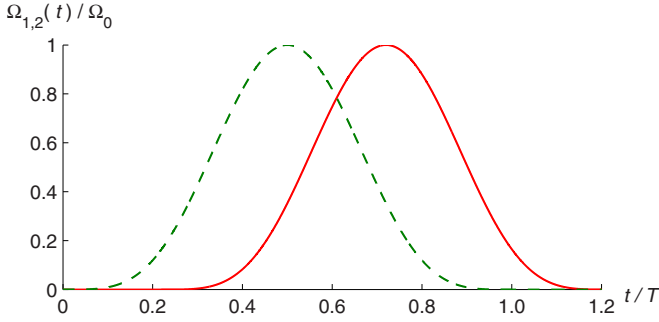
FIG. 2. (Color online) Dependence on t/T of $\Omega_1(t)/\Omega_0$ (solid red line) and $\Omega_2(t)/\Omega_0$ (dashed green line), where $\Omega_1(t)$ and $\Omega_2(t)$ are defined by Eqs. (20) and (21), for the population transfer, with $\tau = 0.22T$.

We remark that, compared to the scheme in Ref. [27], we will prepare the maximal entanglement in the ground states of two atoms, which is robust against the atomic spontaneous emission. Moreover, different from the scheme in Ref. [27], the auxiliary Hamiltonian (17) can serve as a supplement or it can function independently for our time-dependent CDD Hamiltonian. When the auxiliary Hamiltonian functions independently, our system reduces to the interaction between two simple three-level atomic systems and a field mode which could be realized with the current cavity QED technology. Thus, based on the CDD Hamiltonian (17), our proposals for fast population transfer and creation of two-atom maximal entanglement are not sensitive to fluctuations of the experiment parameters. Especially, there is no need to precisely control the operation time in our present scheme.

We now demonstrate that the simultaneous population transfer $|g\rangle_1|f\rangle_2 \to |f\rangle_1|g\rangle_2$ in the two atoms governed by $\tilde{H}(t)$ is much speeded up as compared to the adiabatic passage governed by $H_0(t)$. Let the Rabi frequencies $\Omega_1(t)$ and $\Omega_2(t)$ in the original Hamiltonian $H_0(t)$ depend on time as

$$\Omega_1(t) = \begin{cases} \Omega_0 \sin^4[\pi(t-\tau)/T] & \text{for } \tau \leqslant t \leqslant T+\tau, \\ 0 & \text{otherwise,} \end{cases}$$

(20)

and

$$\Omega_2(t) = \begin{cases} \Omega_0 \sin^4(\pi t/T) & \text{for } 0 \leqslant t \leqslant T, \\ 0 & \text{otherwise,} \end{cases}$$

(21)

with Ω_0 being the pulse amplitude, τ the time delay, and T the operation duration. Figure 2 shows $\Omega_1(t)/\Omega_0$ and $\Omega_2(t)/\Omega_0$ as functions of t/T for a fixed value of the time delay chosen for the best adiabatic passage process. With $\Omega_1(t)$ and $\Omega_2(t)$ defined in (20) and (21), we contrast the performances of population transfer from the initial state $|\phi_1\rangle$ to the target state $|\phi_5\rangle$ based on the adiabatic passage method governed by $H_0(t)$ and on the evolution governed by our auxiliary interaction Hamiltonian $\tilde{H}(t)$ in Fig. 3, where populations $P_k(t) = \langle\phi_k|\rho(t)|\phi_k\rangle$, with $\rho(t)$ being the density matrix associated with the governing Hamiltonian, are plotted versus gt for a given operation duration. The result obviously reveals that near-perfect population transfer by $\tilde{H}(t)$ can be achieved even in a short evolution time [see Fig. 3(a)] for which
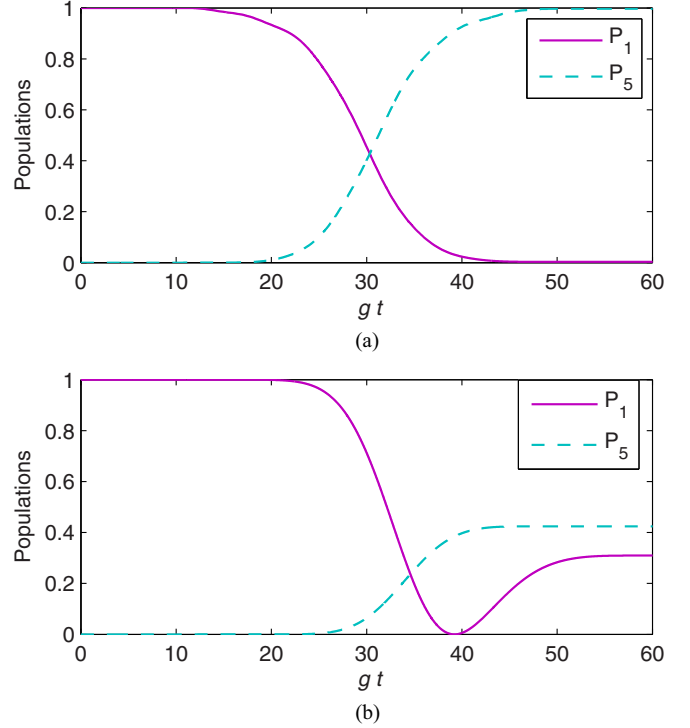

FIG. 3. (Color online) Dependence on gt of the populations $P_1(t)$ and $P_5(t)$ governed by (a) the auxiliary interaction Hamiltonian $\tilde{H}(t)$ with $\Delta_1 = 6g$, $\Delta_2 = 7g$ and (b) the original Hamiltonian $H_0(t)$. In both (a) and (b) the Rabi frequencies $\Omega_1(t)$ and $\Omega_2(t)$ are defined by Eqs. (20) and (21) with $\Omega_0 = 0.2g$, $T = 50/g$, and $\tau = 0.22T$.

the adiabatic passage method breaks down [see Fig. 3(b)]. This means that $\tilde{H}(t)$ indeed provides a shortcut to the adiabatic passage.

In Fig. 4, we plot the fidelity $F(T+\tau) = (\text{Tr}\sqrt{\rho_f^{1/2}\rho(T+\tau)\rho_f^{1/2}})^2$, with ρ_f being the density matrix of the ideal final state and $\rho(T+\tau)$ being that of the evolved state at the end of the pulse operation, as a
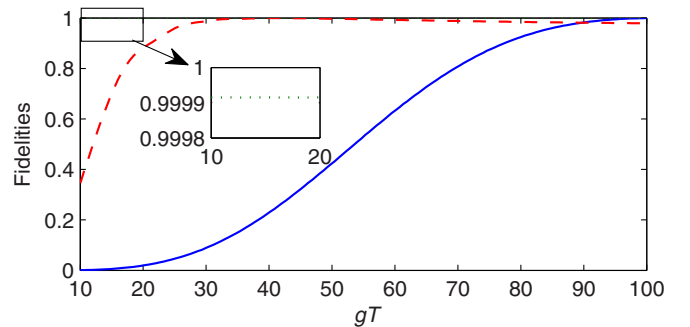

FIG. 4. (Color online) Dependence on gT of the fidelities of the evolved state with respect to the target state using adiabatic passage governed by the Hamiltonian $H_0(t)$ (solid blue line), by the dynamics governed by the CDD Hamiltonian $H_1(t)$ (dotted green line), and by the auxiliary interaction Hamiltonian $\tilde{H}(t)$ (dashed red line) with $\Delta_1 = 6g$ and $\Delta_2 = 7g$ for the case of population transfer. The Rabi frequencies $\Omega_1(t)$ and $\Omega_2(t)$ are defined by Eqs. (20) and (21) with $\Omega_0 = 0.2g$ and $\tau = 0.22T$.

function of the operation time T, by using the original Hamiltonian $H_0(t)$, the CDD Hamiltonian $H_1(t)$, and the auxiliary interaction Hamiltonian $\tilde{H}(t)$. While $H_1(t)$ formally yields a near-perfect population transfer within an arbitrarily short time, $\tilde{H}(t)$ needs a finite operation time to complete the population transfer. This is because $\tilde{H}_{\text{eff}}(t)$ is valid only under the large-detuning condition, which requires longer evolution time to achieve a full population transfer than that required in the resonant-driving CDD Hamiltonian $H_1(t)$. For example, here the fidelity of the evolved state would be higher than 98% when $T \geqslant 30/g$. As for the adiabatic passage evolution via $H_0(t)$, it requires much more time to finish the population transfer: it is about three times longer than that required by $\tilde{H}(t)$.

IV. SHORTCUT FOR MAXIMAL ENTANGLEMENT CREATION BETWEEN TWO ATOMS

Under the weak-driving condition in Eq. (7), one should tailor the two Rabi frequencies $\Omega_1(t)$ and $\Omega_2(t)$ so that at the beginning of the operation $\Omega_1(t)/\Omega_2(t) \to 0$ but at the end $\Omega_1(t)/\Omega_2(t) \to 1$. Such requirements can be met by

$$\Omega_1(t) = \frac{1}{2}\Omega_0' \exp \frac{-[t - (\theta + 1/2)T]^2}{w^2 T^2} \quad (22)$$

and

$$\Omega_2(t) = \Omega_0' \left[\exp \frac{-[t + (\theta - 1/2)T]^2}{w^2 T^2} \right.$$
$$\left. + \frac{1}{2} \exp \frac{-[t - (\theta + 1/2)T]^2}{w^2 T^2} \right], \quad (23)$$

with Ω_0' the pulse amplitude and T the operation duration, while θ and w are some parameters to be chosen for the best performance of the adiabatic passage process. The time dependences of $\Omega_1(t)/\Omega_0'$ and $\Omega_2(t)/\Omega_0'$ are shown in Fig. 5 versus t/T for fixed values of θ and w. With such tailored $\Omega_1(t)$ and $\Omega_2(t)$, we plot in Fig. 6 the evolution of populations $P_{1,5}(t)$, based on the dynamics governed by the interaction Hamiltonian $\tilde{H}(t)$, Fig. 6(a), and on the adiabatic passage governed by the original Hamiltonian $H_0(t)$, Fig. 6(b). From Fig. 6(a), we see that at $t \simeq 30/g$ the interaction Hamiltonian $\tilde{H}(t)$ already yields $P_1(t) \approx P_5(t) = 1/2$. That is, the system
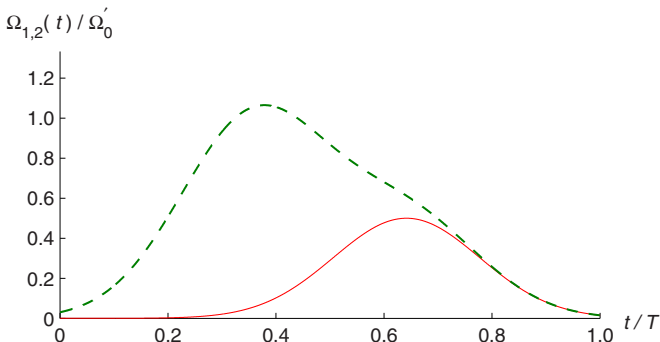

FIG. 5. (Color online) $\Omega_1(t)/\Omega_0'$ (solid red line) and $\Omega_2(t)/\Omega_0'$ (dashed green line) versus t/T for the creation of maximal entanglement between two atoms, where $\Omega_1(t)$ and $\Omega_2(t)$ are defined by Eqs. (22) and (23) with $\theta = 17/120$ and $w = 23/120$.
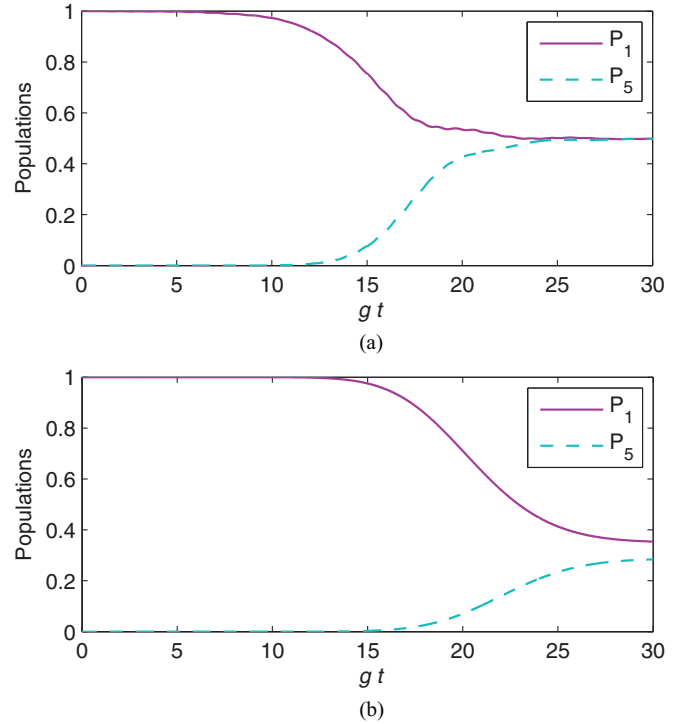

FIG. 6. (Color online) Dependence on gt of the populations $P_1(t)$ and $P_5(t)$ governed by (a) the auxiliary interaction Hamiltonian $\tilde{H}(t)$ with $\Delta_1 = 6g$, $\Delta_2 = 7g$ and (b) the original Hamiltonian $H_0(t)$. In both (a) and (b) the Rabi frequencies $\Omega_1(t)$ and $\Omega_2(t)$ are defined by Eqs. (22) and (23) with $\Omega_0' = 0.3g$, $\theta = 17/120$, $w = 23/120$, and $T = 30/g$.

state at $t \simeq 30/g$ becomes $(-i|\phi_1\rangle + |\phi_5\rangle)/\sqrt{2}$, signifying creation of the atoms' maximal entangled state

$$|\Phi\rangle_{12} = \frac{1}{\sqrt{2}}(-i|g\rangle_1|f\rangle_2 + |f\rangle_1|g\rangle_2). \quad (24)$$

From Fig. 6(b), however, governed by the original Hamiltonian $H_0(t)$, $P_1(t \simeq 30/g)$ is still quite bigger than $P_5(t \simeq 30/g)$.

In Fig. 7 we also plot the fidelities of the evolved states governed by $\tilde{H}(t)$ and $H_0(t)$, with respect to the maximally entangled state $|\Phi\rangle_{12}$, as functions of the operation duration T. Clearly from Fig. 7, to obtain the maximum entanglement between the two atoms, a much longer operation time is required by the adiabatic passage method than that by $\tilde{H}(t)$. Thus, the results in Figs. 6 and 7 confirm that $\tilde{H}(t)$ indeed accelerates the creation of maximally entangled states for the two atoms as compared to the original Hamiltonian $H_0(t)$. Or, in other words, the dynamics governed by $\tilde{H}(t)$ is a nonadiabatic shortcut to adiabaticity governed by $H_0(t)$ for creation of maximal entanglement between two atoms within a cavity.

V. ROBUSTNESS OF THE SHORTCUT SCHEMES

Not only speed but also robustness against possible mechanisms of decoherence is important for a scheme to be applicable in quantum-information processing and quantum computing. In the problems of our concern here decoherences may originate from the atomic spontaneous emission and the
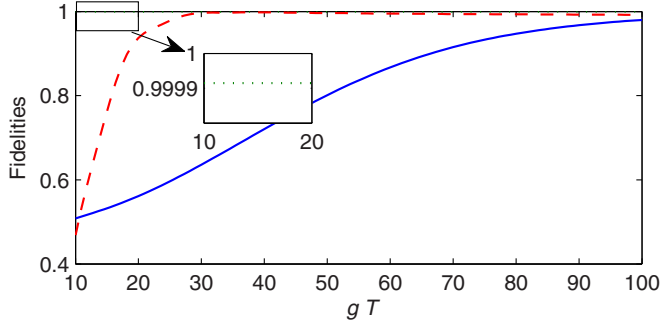
FIG. 7. (Color online) Dependence on gT of the fidelities of the evolved state with respect to the target state using adiabatic passage governed by the Hamiltonian $H_0(t)$ (solid blue line), the dynamics governed by the CDD Hamiltonian $H_1(t)$ (dotted green line), and by the auxiliary interaction Hamiltonian $\tilde{H}(t)$ (dashed red line) with $\Delta_1 = 6g$, $\Delta_2 = 7g$ for the case of maximal entanglement creation. The Rabi frequencies $\Omega_1(t)$ and $\Omega_2(t)$ are defined by Eqs. (22) and (23) with $\Omega_0' = 0.3g$, $\theta = 17/120$, and $w = 23/120$.

cavity decay. To examine robustness of our shortcut schemes described in the previous sections against such decoherence mechanisms we numerically solve the master equation for the whole system's density matrix $\rho(t)$, which has the form

$$
\begin{aligned}
\partial_t \rho(t) = &-i[H_0(t) + \tilde{H}(t), \rho(t)] \\
&- \frac{\kappa_a}{2}[a^\dagger a \rho(t) - 2a\rho(t)a^\dagger + \rho(t)a^\dagger a] \\
&- \frac{\kappa_b}{2}[b^\dagger b \rho(t) - 2b\rho(t)b^\dagger + \rho(t)b^\dagger b] \\
&- \sum_{k=1}^{2} \sum_{m=g,f} \sum_{n=s,e} \frac{\Gamma_{nm}^k}{2}\big[S_{mn}^{k+} S_{mn}^k \rho(t) \\
&- 2S_{mn}^k \rho(t) S_{mn}^{k+} + \rho(t) S_{mn}^{k+} S_{mn}^k\big],
\end{aligned}
\tag{25}
$$

where κ_a (κ_b) is the photon leakage rate of the cavity mode a (b), Γ_{nm}^k is the kth atom's spontaneous emission rate from the excited state $|n\rangle_k$ to the ground state $|m\rangle_k$ and $S_{mn}^k = |m\rangle_k\langle n| = S_{nm}^{k+}$. For simplicity, we assume $\Gamma_{nm}^k = \Gamma/2$ and $\kappa_a = \kappa_b = \kappa$ in numerically solving the master equation (25) with the initial condition $\rho(0) = |\phi_1\rangle\langle\phi_1|$. In Fig. 8, we display the dependence on the ratios Γ/g and κ/g of the fidelities of the evolved state at the end of the operation time for the population transfer [Fig. 8(a)] and the creation of maximal entanglement [Fig. 8(b)]. The physical configuration that we consider in the present scheme employs electric dipole transitions on the D_1 line of a single ^{87}Rb atom [29]. In a real experiment, one can couple this atom simultaneously to two optical cavity modes and two laser fields. Two stable hyperfine ground states are the $(F = 1, m = -1)$ level and the $(F = 2, m = -2)$ level of the $5^2 S_{1/2}$ state, while two metastable hyperfine excited states are the $(F' = 1, m = -1)$ level and the $(F' = 2, m = -2)$ level of $5^2 P_{1/2}$. The related cavity-QED parameters could be achievable with, for example, microtoroidal whispering-gallery-mode resonators [30]. In current experiments, the parameters $g = 2.5$ GHz, $\kappa = 10$ MHz, and $\Gamma = 10$ MHz have been reported in Refs. [30,31]. For such parameters, we can see from Fig. 8 that fidelities higher than 98% can be achieved in
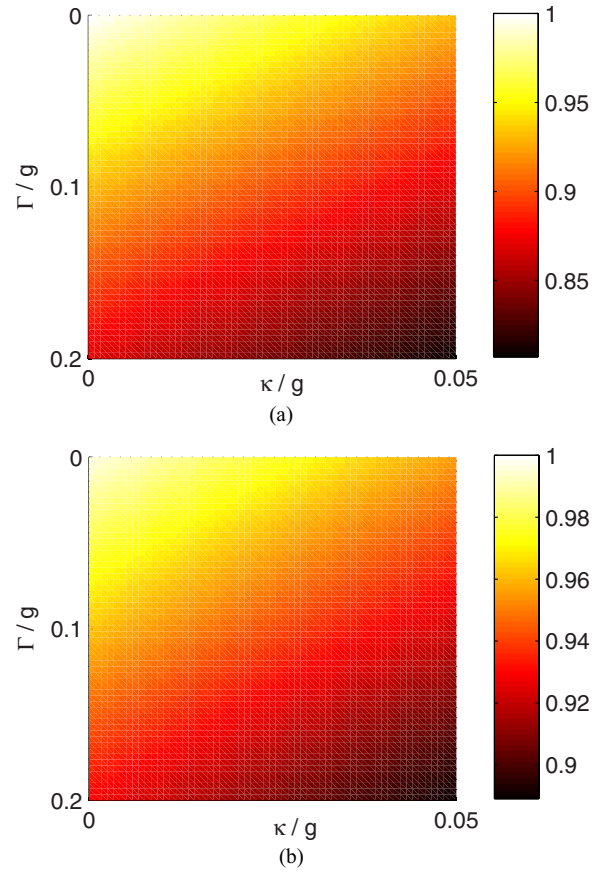

(a)

(b)

FIG. 8. (Color online) Dependences on Γ/g and κ/g of the fidelities of the evolved state at the end of the operation time with respect to the target state that are obtained by numerically solving the master equation (15) for (a) the population transfer with $\Omega_1(t)$ and $\Omega_2(t)$ defined by Eqs. (20) and (21) with $\Omega_0 = 0.2g$, $T = 50/g$, and $\tau = 0.22T$ and (b) the maximal entanglement creation with $\Omega_1(t)$ and $\Omega_2(t)$ defined by Eqs. (22) and (23) with $\Omega_0' = 0.3g$, $\theta = 17/120$, $w = 23/120$, and $T = 30/g$.

both the shortcut schemes. Therefore, the schemes are robust and might be promising within the current technology.

VI. CONCLUSION

In conclusion, we propose nonadiabatic shortcut schemes for the population transfer and creation of maximal entanglement between two atoms based on the CQED that perform much faster than those based on the adiabatic passage method. Using the transitionless driving approach, we analytically derive a CDD Hamiltonian, the shortcut performance of which is numerically demonstrated to be equivalent to our auxiliary interaction Hamiltonian under a large detuning regime. The speed in both the population transfer and the maximal entanglement creation between two atoms can be improved by about three times those based on the conventional adiabatic passage. Also, the present schemes are shown to be robust against the decoherences caused by the atomic spontaneous emission and cavity decay.

[1] M. V. Berry, J. Phys. A **42**, 365303 (2009).
[2] J. R. Kuklinski, U. Gaubatz, F. T. Hioe, and K. Bergmann, Phys. Rev. A **40**, 6741 (1989).
[3] X. Chen and J. G. Muga, Phys. Rev. A **86**, 033405 (2012).
[4] X. Chen, A. Ruschhaupt, S. Schmidt, A. del Campo, D. Guéry-Odelin, and J. G. Muga, Phys. Rev. Lett. **104**, 063002 (2010).
[5] D. Stefanatos, J. Ruths, and J. S. Li, Phys. Rev. A **82**, 063422 (2010).
[6] K. H. Hoffmann, P. Salamon, Y. Rezek, and R. Kosloff, Euro. Phys. Lett. **96**, 60015 (2011).
[7] A. Rahmani and C. Chamon, Phys. Rev. Lett. **107**, 016402 (2011).
[8] E. Torrontegui, S. Ibanez, X. Chen, A. Ruschhaupt, D. Guery-Odelin, and J. G. Muga, Phys. Rev. A **83**, 013415 (2011).
[9] S. Ibanez, S. Martinez-Garaot, X. Chen, E. Torrontegui, and J. G. Muga, Phys. Rev. A **84**, 023415 (2011).
[10] E. Torrontegui, X. Chen, M. Modugno, S. Schmidt, A. Ruschhaupt, and J. G. Muga, New J. Phys. **14**, 013031 (2012).
[11] Y. Li, L. A. Wu, and Z. D. Wang, Phys. Rev. A **83**, 043804 (2011).
[12] A. del Campo, Phys. Rev. A **84**, 031606(R) (2011).
[13] A. del Campo, M. G. Boshier, Sci. Rep. **2**, 648 (2012).
[14] X. Chen, I. Lizuain, and A. Ruschhaupt, D. Guéry-Odelin, and J. G. Muga, Phys. Rev. Lett. **105**, 123003 (2010).
[15] X. Chen, E. Torrontegui, and J. G. Muga, Phys. Rev. A **83**, 062116 (2011).
[16] J. G. Muga, X. Chen, S. lbáñez, I. Lizuain, and A. Ruschhaupt, J. Phys. B **43**, 085509 (2010).
[17] A. Ruschhaupt, X. Chen, D. Alonso, and J. G. Muga, New J. Phys. **14**, 093040 (2012).
[18] A. del Campo, Phys. Rev. Lett. **111**, 100502 (2013).
[19] X. Shi and L. F. Wei, arXiv:1309.3020.
[20] M. Lu, L. T. Shen, Y. Xia, and J. Song, arXiv:1305.5458.
[21] J. F. Schaff, X. L. Song, P. Vignolo, and G. Labeyrie, Phys. Rev. A **82**, 033430 (2010).
[22] J. F. Schaff, X. L. Song, P. Capuzzi, P. Vignolo, and G. Labeyrie, Euro. Phys. Lett. **93**, 23001 (2011).
[23] A. Walther, F. Ziesel, T. Ruster, S. T. Dawkins, K. Ott, M. Hettrich, K. Singer, F. Schmidt-Kaler, and U. Poschinger, Phys. Rev. Lett. **109**, 080501 (2012).
[24] R. Bowler, J. Gaebler, Y. Lin, T. R. Tan, D. Hanneke, J. D. Jost, J. P. Home, D. Leibfried, and D. J. Wineland, Phys. Rev. Lett. **109**, 080502 (2012).
[25] S. Y. Tseng and X. Chen, Opt. Lett. **37**, 5118 (2012).
[26] M. G. Bason, M. Viteau, N. Malossi, P. Huillery, E. Arimondo, D. Ciampini, R. Fazio, V. Giovannetti, R. Mannella, and O. Morsch, Nat. Phys. **8**, 147 (2012).
[27] S. B. Zheng and G. C. Guo, Phys. Rev. Lett. **85**, 2392 (2000); S. B. Zheng, Appl. Phys. Lett. **94**, 154101 (2009).
[28] Z. B. Yang, H. Z. Wu, and S. B. Zheng, Eur. Phys. J. D **61**, 737 (2011).
[29] D. A. Steck, Rubidium 87 D Line Data, available online at http://steck.us/alkalidata (revision 2.1.4, 23 December 2010).
[30] S. M. Spillane, T. J. Kippenberg, K. J. Vahala, K. W. Goh, E. Wilcut, and H. J. Kimble, Phys. Rev. A **71**, 013817 (2005).
[31] M. J. Hartmann, F. G. S. L. Brandão, and M. B. Plenio, Nat. Phys. **2**, 849 (2006).